THE JOURNAL OF BIOLOGICAL CHEMISTRY
Vol. 276, No. 14, Issue of April 6, pp. 11323–11334, 2001

Printed in U.S.A.

Regulation of an Endogenous Locus Using a Panel of Designed Zinc Finger Proteins Targeted to Accessible Chromatin Regions

ACTIVATION OF VASCULAR ENDOTHELIAL GROWTH FACTOR A*

Received for publication, December 12, 2000
Published, JBC Papers in Press, January 5, 2001, DOI 10.1074/jbc.M011172200

Pei-Qi Liu‡, Edward J. Rebar‡, Lei Zhang, Qiang Liu, Andrew C. Jamieson, Yuxin Liang, Hong Qi, Pei-Xiang Li, Bingliang Chen, Matthew C. Mendel, Xiaohong Zhong, Ya-Li Lee, Stephen P. Eisenberg§, S. Kaye Spratt, Casey C. Case, and Alan P. Wolffe¶

From Sangamo BioSciences Incorporated, Richmond, California 94804

We have mapped conserved regions of enhanced DNase I accessibility within the endogenous chromosomal locus of vascular endothelial growth factor A (VEGF-A). Synthetic zinc finger protein (ZFP) transcription factors were designed to target DNA sequences contained within the DNase I-hypersensitive regions. These ZFPs, when fused to either VP16 or p65 transcriptional activation domains, were able to activate expression of the VEGF-A gene as assayed by mRNA accumulation and VEGF-A protein secretion through a range exceeding that induced by hypoxic stress. Importantly, multiple splice variants of VEGF-A mRNA with defined physiological functions were induced by a single engineered ZFP transcription factor. We present evidence for an enhanced activation of VEGF-A gene transcription by ZFP transcription factors fused to VP16 and p65 targeted to two distinct chromosomal sites >500 base pairs upstream or downstream of the transcription start site. Our strategy provides a novel approach for dissecting the requirements for gene regulation at a distance without altering the DNA sequence of the endogenous target locus.

A major focus in the study of gene regulation involves the mechanisms by which the cell achieves specific activation of endogenous chromosomal genes. In addressing this issue, rationally designed components of the transcriptional machinery can provide powerful tools for testing our understanding of gene regulation (1–3). In particular, artificial transcription factors, targeted to novel sequences within a given locus and bearing functional domains of the experimenter's choosing, may prove especially useful since they offer the prospect of complete recapitulation of any given activation process using totally defined components. Artificial transcription factors may also provide practical benefits in areas such as medicine and biotechnology.

The DNA-binding motif of choice that has emerged for achieving specific recognition of predetermined, desired DNA sequences is the Cys_2-His_2 zinc finger. Over the past decade, selection and design studies have demonstrated the adaptability of this motif and have yielded simple, powerful strategies for designing zinc finger proteins (ZFPs)[1] that can bind specifically to virtually any DNA sequence (4–15). More recently, ZFPs with engineered DNA sequence specificities have begun to be used as artificial transcription factors to regulate endogenous chromosomal genes (16–18). The growing use of these designed ZFPs has led to an appreciation of the role of chromatin structure in the ability of designed transcription factors to successfully access their target sequences and to function as transcriptional regulators at endogenous loci. In one recent study, a clear discrepancy was noted between the ability of ZFPs to activate transcription from naked reporter DNA and an endogenous chromosomal locus, with only a subset of reporter-active ZFPs successfully up-regulating the endogenous gene (17). Subsequent analysis of chromatin structure suggested site accessibility as the cause of this difference in behavior (17). This study, along with the growing awareness of the role of chromatin remodeling in transcriptional regulation (for example, see Refs. 19–21), highlights the necessity of considering chromatin structure in any use of artificial transcription factors.

Our goal for this study was to identify a panel of ZFPs that could activate the endogenous gene for vascular endothelial growth factor A (VEGF-A). VEGF-A is an endothelial cell-specific mitogen that is a key inducer of new blood vessel growth, both during embryogenesis and in adult processes such as wound healing (for recent reviews, see Refs. 22–24). Its central roles in both vasculogenesis and angiogenesis apparently necessitate the control of VEGF-A expression levels by precise regulatory mechanisms. Mouse studies have highlighted VEGF-A as a clear example of a gene whose haploinsufficiency causes embryonic lethality (25, 26). Furthermore, several studies have suggested that proper VEGF-A function requires expression of appropriate relative levels of the major splice variants produced by this gene (27, 28). A diversity of conditions and transcription factors have been implicated as inducing VEGF-A expression (29–35), of which perhaps the best characterized is the hypoxic response, mediated by hypoxia-inducible factor 1 (36–40). Consistent with its highly regulated nature, VEGF-A dysregulation plays a role in a variety of medical conditions, including tumor growth, diabetic

* The costs of publication of this article were defrayed in part by the payment of page charges. This article must therefore be hereby marked "*advertisement*" in accordance with 18 U.S.C. Section 1734 solely to indicate this fact.

‡ These authors contributed equally to this work.

§ Present address: Bolder Biotechnology, Inc., Campus Box 347, C.U.-Boulder, Boulder, CO 80309-0347.

¶ To whom correspondence should be addressed: Sangamo BioSciences Inc., Point Richmond Tech Center, 501 Canal Blvd., Suite A100, Richmond, CA 94804. Tel.: 510-970-6000 (ext. 216); Fax: 510-236-8951; E-mail: awolffe@sangamo.com.

[1] The abbreviations used are: ZFPs, zinc finger proteins; VEGF-A, vascular endothelial growth factor A; HEK293, human embryonic kidney 293; NF-κB, nuclear factor κB; bp, base pair(s); PCR, polymerase chain reaction; RT-PCR, reverse transcription-polymerase chain reaction; ELISA, enzyme-linked immunosorbent assay.

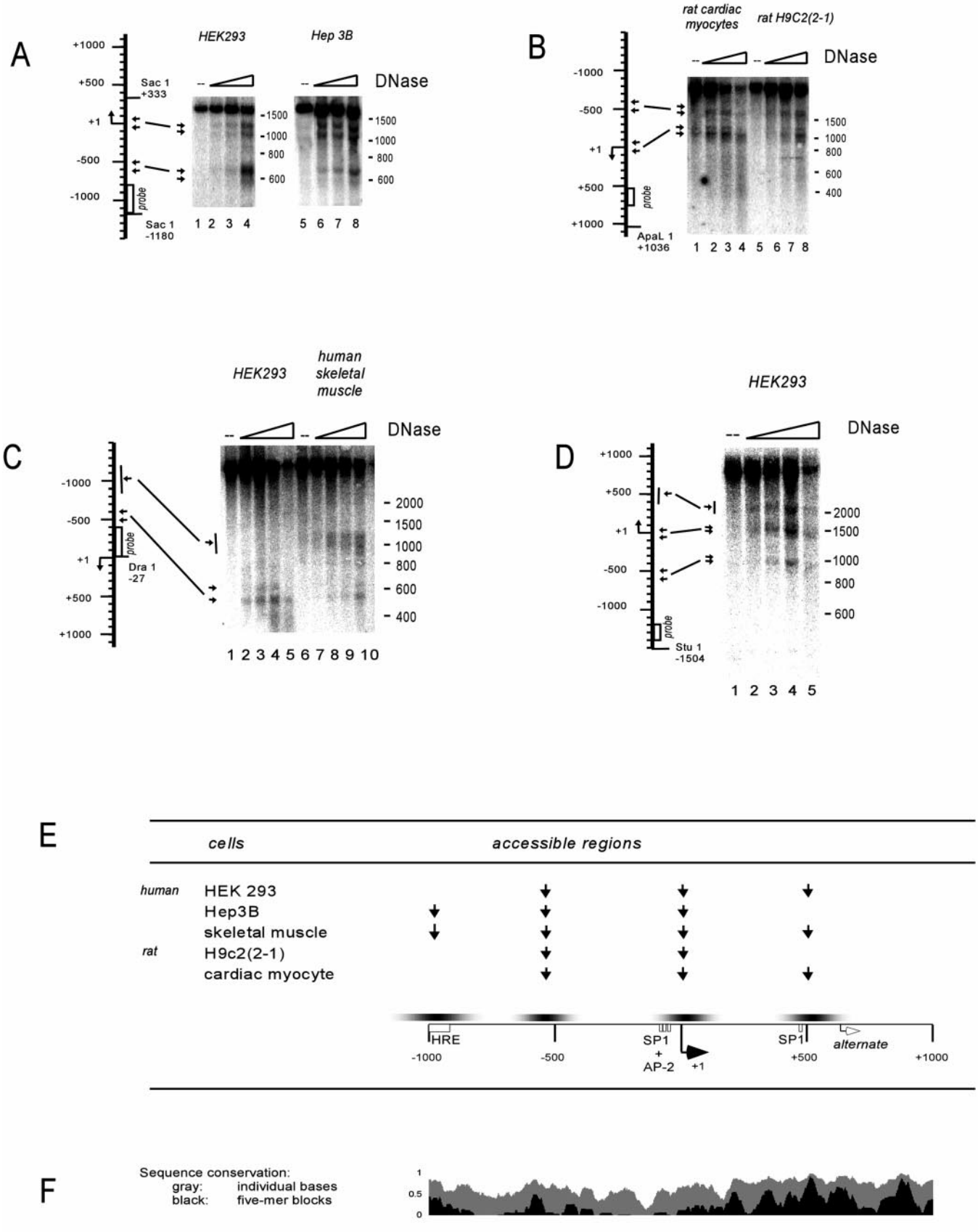

FIG. 1. **Regions of enhanced chromatin accessibility in the promoter of VEGF-A.** *A* and *B*, constitutive sites. Nuclei from the indicated human (*A*) or rat (*B*) cells were partially digested with DNase I (see "Experimental Procedures"), followed by Southern blot analysis using the indicated restriction enzymes and probes. *Vertical bars* represent genomic DNA in the VEGF-A promoter region. *Bent arrows* denote the transcription start site, and *tick marks* indicate units of 100 bp. Positions of restriction enzyme target sites are indicated in base pairs relative to the start site of VEGF-A transcription. The migration pattern for a set of DNA standard fragments is indicated to the right of each *panel*, with the size of each fragment given in base pairs. *Arrows* highlight the relationship of the observed bands to the location of accessible chromatin regions relative to the transcription start sites of VEGF-A. DNase I concentrations were as follows: *A*, HEK293 nuclei (*lanes 1–4*), 0, 7.5, 15, and 60

TABLE I
Nucleotide sequences of the primers and probes used for Taqman analysis

Primer/probe name	Nucleotide sequences (5′ to 3′)
VEGF-A forward primer	5′-GTGCATTGGAGCCTTGCCTTG-3′
VEGF-A reverse primer	5′-ACTCGATCTCATCAGGGTACTC-3′
VEGF-A Taqman probe	5′-FAM-CAGTAGCTGCGCTGATAGACATCCA-TAMRA-3′
GAPDH[a] forward primer	5′-CCATGTTCGTCATGGGTGTGA-3′
GAPDH reverse primer	5′-CATGGACTGTGGTCATGAGT-3′
GAPDH Taqman probe	5′-FAM-TCCTGCACCACCAACTGCTTAGCA-TAMRA-3′
18 S RNA forward primer	5′-TTCCGATAACGAACGAGACTCT-3′
18 S RNA reverse primer	5′-TGGCTGAACGCCACTTGTC-3′
18 S RNA Taqman probe	5′-FAM-TAACTAGTTACGCGACCCCCGAG-TAMRA-3′
VP16-FLAG forward primer	5′-CATGACGATTTCGATCTGGA-3′
VP16-FLAG reverse primer	5′-CTACTTGTCATCGTCGTCCTTG-3′
VP16-FLAG Taqman probe	5′-FAM-ATCGGTAAACATCTGCTCAAACTCGA-TAMRA-3′

[a] GAPDH, glyceraldehyde-3-phosphate dehydrogenase.

retinopathy, and ischemic heart and limb diseases. Consequently, VEGF-A would appear to provide an attractive target for both pro- and anti-angiogenic gene therapies using designed artificial transcription factors.

In this study, we have made use of engineered Cys_2-His_2 ZFPs and knowledge of chromosomal structure to achieve activation of the endogenous chromosomal locus containing the gene for VEGF-A. We first used DNase I hypersensitivity mapping analysis to identify accessible regions of the VEGF-A locus conserved across a variety of cell lines from man and rat. This analysis identified four distinct DNase I-accessible regions, of which three were present in the HEK293 cells used for activation studies. Novel ZFPs targeted to sites within the HEK293-specific DNase I-accessible regions were then characterized with respect to their DNA-binding properties and ability to activate VEGF-A expression. We found that each of our designed ZFPs bound its intended target with an apparent K_d of <3 nM and, when linked to the VP16 transcriptional activation domain (41), activated transcription of both the endogenous VEGF-A gene and a transiently transfected native reporter construct containing ~3 kilobases of the VEGF-A promoter. We also linked our ZFPs to the activation domain from the p65 subunit of NF-κB (42) and tested for the capacity to activate transcription of endogenous VEGF-A both alone and in certain combinations with our VP16-linked ZFPs.

We found that this strategy yielded eight distinct ZFPs targeted to seven 9-bp sites that activated VEGF-A expression and that, for certain ZFPs, linkage to activation domains from either VP16 or p65 provided differing levels of activation depending on the chromosomal site that is targeted. Furthermore, when certain combinations of our VP16- and p65-linked ZFPs targeted to distinct chromosomal sites were cotransfected, the observed VEGF-A activation was more than additive relative to the activation levels of the individual ZFPs. Finally, we show that the levels of activation achieved by these engineered transcription factors exceeded VEGF-A levels attained during the hypoxic response and that the relative proportions of VEGF-A splice variants produced by this activation closely approximated normal splice variant ratios seen in these cells.

EXPERIMENTAL PROCEDURES

Mapping of DNase I-accessible Chromatin Regions in the VEGF-A Locus—The immortalized cell lines used in these studies (HEK293, Hep3B, and H9c2(2-1)) were obtained from American Type Culture Collection, and human primary skeletal muscle cells were obtained from Clonetics Corp. Each line was maintained essentially as recommended by the suppliers. Rat primary cardiac myocytes were recovered from the hearts of day 1 neonatal Wistar-Han rats (Charles River Laboratories) via dissociation with a solution of 115 units/ml type II collagenase and 0.08% pancreatin. They were then purified on a discontinuous Percoll gradient, resuspended in plating medium containing 15% serum, and plated on gelatin-coated plates for 24 h. Cells were maintained in serum-free medium for 24–48 h prior to use in DNase I mapping studies.

Nuclei were isolated and treated with DNase I (Worthington) essentially as described (17), except that DNase I digests were carried out for 1.5 min at 22 °C, and the concentrations of DNase I used were as indicated in the legend to Fig. 1. Genomic DNA isolation, restriction enzyme digestion, and Southern blot analysis were then performed essentially as described (17), except that enzymes and probes were as indicated in Fig. 1.

Synthesis, Purification, and Gel Shift Analysis of Zinc Finger Proteins—Genes encoding our VEGF-A-targeted ZFPs were assembled, cloned, and purified as previously described (17). Briefly, oligonucleotides encoding α-helix and β-sheet regions of each three-finger protein were assembled using PCR (see Fig. 2, *A* and *B*), and each resultant ZFP gene was cloned into the pMal-c2 plasmid (New England Biolabs Inc.) as a fusion with DNA encoding maltose-binding protein. Maltose-binding protein-ZFP fusions were then expressed and affinity-purified using an amylose resin (New England Biolabs Inc.).

Binding studies were performed essentially as described (17), except that the binding reactions contained ~10 pM labeled target site, and the buffer composition was as follows: 17 mM Tris, 170 mM KCl, 1.7 mM $MgCl_2$, 3.5 mM dithiothreitol, 0.033 mM $ZnCl_2$, 15% glycerol, 300 μg/ml bovine serum albumin, and 0.03% IGEPAL. In addition, ZFP concentrations for these studies were determined directly by measuring the DNA-binding activity of each ZFP preparation using conditions under which binding is essentially stoichiometric (concentrations of ZFP and

units/ml; and Hep3B nuclei (*lanes 5–8*), 0, 7.5, 15, and 30 units/ml. *B*, rat cardiac myocyte nuclei (*lanes 1–4*), 0, 3.75, 7.5, and 15 units/ml; and rat H9c2(2-1) nuclei (*lanes 5–8*), 0, 15, 30, and 60 units/ml. *C*, presence of an accessible region ~1000 bp upstream of the VEGF-A transcription start site in primary skeletal muscle cells, but not in HEK293 cells. Details were as described for *A* and *B*, except that nuclei were isolated from HEK293 cells or human primary skeletal muscle cells. DNase I concentrations were as follows: HEK293 nuclei (*lanes 1–5*), 0, 7.5, 15, 30, and 60 units/ml; and human primary skeletal muscle nuclei (*lanes 6–10*), 0, 3.75, 7.5, 15, and 30 units/ml. *D*, presence of an accessible region 500 bp downstream of the VEGF-A transcription start site in HEK293 cells. Details were as described for *A* and *B*. DNase I concentrations were as follows: 0, 15, 30, 60, and 120 units/ml (*lanes 1–5*, respectively). *E*, summary of DNase I-accessible regions observed in our studies. The cell types tested are indicated on the left. Observation of a particular open region in a given cell type is denoted by an *arrow*. The −550 and +1 hypersensitive regions occurred in all cell types tested, whereas the −1000 and +500 sites appeared only in a subset of tested cells. A schematic representation of the VEGF-A promoter, encompassing bases −1000 to +1000 relative to the principal transcription start site, is provided on the bottom. The *black arrow* denotes the principal site of transcription initiation, whereas the position of a reported alternate start site (47) is highlighted by the *white arrow*. Key regulatory elements are also shown (hypoxia response element (*HRE*)). DNase I-accessible regions are indicated by *gradient-shaded rectangles*. *F*, sequence conservation among man, mouse, and rat in the promoter region of VEGF-A. Each *point* in the *gray profile* indicates the fractional conservation of human VEGF-A sequence in both rat and mouse within a 50-bp window centered on that point. The *black profile* is identical, except that it indicates the fractional conservation of 5-bp blocks.

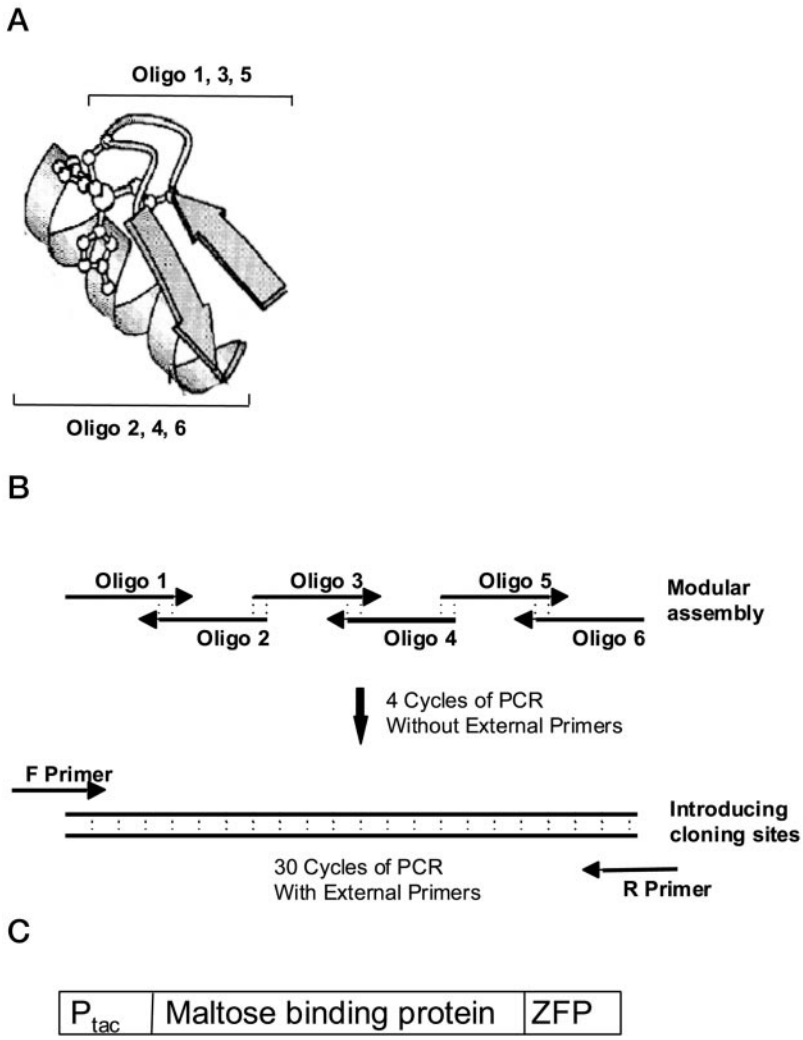

FIG. 2. **Construction scheme and DNA-binding properties of the VEGF-A targeted ZFPs.** *A*, ribbon diagram of the x-ray crystal structure of an individual zinc finger with two β-sheets linked to the DNA-binding α-helix (61). The locations of oligonucleotide primers used for assembly are indicated relative to the regions of the finger they encode. In our ZFP assembly scheme, oligonucleotides (*Oligo*) 1, 3, and 5 comprise the β-sheet regions, and oligonucleotides 2, 4, and 6 comprise the DNA-binding α-helix regions. *B*, assembly scheme of the ZFPs. Six overlapping oligonucleotides were annealed and amplified with a pair of external oligonucleotides. The PCR products were then cloned into the *Kpn*I and *Bam*HI sites of the pMal-c2 bacterial expression vector. *C*, scheme of the maltose-binding protein-ZFP fusions used for gel shift analysis. *D*, schematic representation of the human VEGF-A gene showing the locations of the principal (*black arrow*) and a reported alternate (*white arrow*) (47) transcription initiation site, DNase I-accessible regions in HEK293 cells (*gradient-filled rectangles*), and target site locations for the ZFPs used in these studies (*white vertical rectangles*). The location of the upstream edge of each ZFP target is indicated by the number below it. Numbering is relative to the start site of transcription (+1). *E*, gel shift assays using the various VEGF-A-targeted ZFPs binding to their DNA targets. A 2-fold dilution series of each protein was tested for binding to its DNA target, with the highest concentration in the *second lane* and the lowest concentration in the *eleventh lane* (from left to right). The *first lane* is a control lane containing probe alone.

target site $> 50 \times K_d$). Using this modified protocol, SP1 exhibits a significantly higher apparent affinity than was determined in previous studies (17), and it is likely that the use of both activity-based estimates of ZFP concentration and the new binding buffer in these studies contributed to the difference in apparent K_d values.

Zinc Finger Protein Expression Constructs Used for Cell Culture Studies—ZFPs with distinct binding properties were assembled and cloned into the pcDNA3 mammalian expression vector (Invitrogen) as described previously (17). A cytomegalovirus promoter drove the expression of all the ZFPs in mammalian cells. All ZFP constructs contained an N-terminal nuclear localization signal (Pro-Lys-Lys-Lys-Arg-Lys-Val) from SV40 large T antigen, a ZFP DNA-binding domain, an activation domain, and a FLAG peptide (Asp-Tyr-Lys-Asp-Asp-Asp-Asp-Lys). ZFP-VP16 fusions contained the herpes simplex virus VP16 activation domain from amino acids 413–490 (17, 41). ZFP-p65 fusions contained the human NF-κB transcription factor p65 subunit (amino acids 288–548) as the activation domain (42).

Assay for Human VEGF-A Reporter Activation—The effect of ZFPs on human VEGF-A promoter activity was measured using a luciferase reporter construct containing the human VEGF-A promoter. The human VEGF-A-luciferase reporter pGLPVFH was made by inserting a genomic DNA fragment containing 3318 bp of the human VEGF-A promoter and its flanking sequences (nucleotides −2279 to +1039) into the pGL3-basic vector (Promega) between the *Kpn*I and *Nco*I sites. The translation start codon ATG of the VEGF-A gene was directly fused with the luciferase gene in this construct. HEK293 cells were grown in Dulbecco's modified Eagle's medium supplemented with 10% fetal bovine serum in a 5% CO_2 incubator at 37 °C. Cells were plated in 24-well plates at a density of 160,000 cells/well 1 day before transfection. The VEGF-A reporter construct and ZFP-VP16 fusion plasmid were cotransfected into the cells via LipofectAMINE reagent (Life Technologies, Inc.) according to the manufacturer's recommendations, using 1.5 μl of LipofectAMINE reagent, 260 ng of the VEGF-A reporter construct, 30 ng of plasmid DNA encoding ZFP-VP16, and 10 ng of the pRL-CMV control plasmid (Promega). The medium was removed and replaced with fresh medium 16 h after transfection. Forty hours after transfection, the medium was removed, and the cells were harvested and assayed for luciferase reporter activity using the dual-luciferase assay system (Promega) according to the manufacturer's protocol.

Assay for Activity of ZFP Fusions for Endogenous VEGF-A Activation in Human Cells by Transient Transfection—HEK293 cells were plated in 24-well plates at a density of 160,000 cells/well and grown as described above. One day later, plasmids encoding ZFP-VP16 fusions were transfected into the cells via LipofectAMINE reagent according to the manufacturer's recommendations, using 1.5 μl of LipofectAMINE reagent and 0.3 μg of ZFP plasmid DNA per well. The medium was removed and replaced with fresh medium 16 h after transfection. Forty hours after transfection, the culture medium and the cells were harvested and assayed for VEGF-A expression. VEGF-A protein contents in the culture medium were assayed using a human VEGF-A ELISA kit (R&D Systems) according to the manufacturer's protocol.

For Western analysis of ZFP protein expression, cells were lysed with Laemmli sample loading buffer, and the lysates were analyzed via electrophoresis on a 10% polyacrylamide gel (Bio-Rad) followed by Western blotting using anti-FLAG M2 monoclonal antibody (Sigma), which recognizes the FLAG epitope tag of the engineered ZFPs. The Western blots were visualized by ECL (Amersham Pharmacia Biotech) as described previously (17).

For quantitative RT-PCR analysis of VEGF-A mRNA levels, the cells were lysed, and total RNA was prepared using the RNeasy total RNA isolation kit with in-column DNase treatment (QIAGEN Inc.). RNA (25 ng) was used in real-time quantitative RT-PCR analysis using Taqman chemistry on an ABI 7700 SDS machine (PerkinElmer Life Sciences) as described previously (17). Briefly, reverse transcription was performed at 48 °C for 30 min using MultiScribe reverse transcriptase (PerkinElmer Life Sciences). Following a 10-min denaturation at 95 °C,

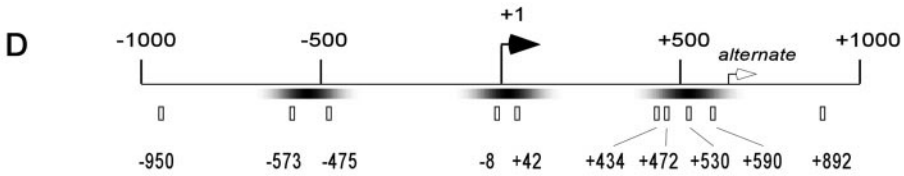

E

ZFP	Target	Gel Shift	Apparent Kd (nM)
VZ-950	GAAGAGGACc	Bound / Free	0.18
VZ-573	GGGGGCGCTc	Bound / Free	0.63
VZ-475	GTGTGGGGTt	Bound / Free	0.35
SP1	GGGGCGGGGg	Bound / Free	0.25
VZ-8	GGGGAGGATc	Bound / Free	2.83
VZ+42 / +530	GCTGGGGGCt	Bound / Free	0.33
VZ+434a	GGGGGTGACc	Bound / Free	0.14
VZ+434b	GGGGGTGACc	Bound / Free	0.41
VZ+472	AAGGGGGAGg	Bound / Free	0.005
VZ+590	GCAGGGGCCg	Bound / Free	0.23
VZ+892	GCTGGAGCAc	Bound / Free	0.24

FIG. 2—continued

PCR amplification using AmpliGold DNA polymerase was conducted for 40 cycles at 95 °C for 15 s and at 60 °C for 1 min. The results were analyzed using SDS Version 1.6.3 software. The primers and probes used for Taqman analysis are listed in Table I. The primers and probes used for human VEGF-A recognize all known splice variants.

Northern and Splice Variants Analyses—HEK293 cells were grown in 150-mm dishes and transfected with the pcDNA3 control vector or ZFP using LipofectAMINE reagent according to the manufacturer's recommendations. Cells and conditioned medium were harvested 40 h after transfection. Total RNA was extracted from the cells using Trizol reagent (Life Technologies, Inc.) followed by an RNeasy total RNA isolation midi-prep system (QIAGEN Inc.). For Northern analysis of VEGF-A mRNA expression, various total RNA samples (30 μg) were resolved on a 1.2% formaldehyde-agarose gel and blotted onto a Nytran SuperCharge membrane (Schleicher & Schüll). The membrane was hybridized to a ^{32}P-labeled human VEGF-A-165 cDNA antisense riboprobe at 68 °C in Ultrahyb™ hybridization buffer (Ambion, inc.). After washing with 0.1× SSC and 0.1% SDS at 68 °C, the membrane was exposed to film. The same membrane was stripped by boiling in 0.1% SDS and rehybridized with a human β-actin antisense riboprobe.

For analysis of multiple splice variants, total RNA samples (0.5 μg) were subjected to 20-cycle RT-PCR using a Titan™ one-tube RT-PCR system (Roche Molecular Biochemicals). The primers used were 5′-ATGAACTTTCTGCTGTCTTGGGTGCATT-3′ and 5′-TCACCGC-CTCGGCTTGTCACAT-3′. The PCR products were resolved on a 3% Nusieve 3:1 agarose gel (FMC Corp. BioProducts), blotted onto a Nytran SuperCharge membrane, and analyzed by Southern hybridization to a ^{32}P-labeled human VEGF-A cDNA probe that recognizes all splice variants. The expected PCR product sizes for VEGF-A-189, VEGF-A-165, and VEGF-A-120 were 630, 576, and 444 bp, respectively.

RESULTS

Constitutive and Cell-specific Regions of Accessible Chromatin in the VEGF-A Locus—Our chromatin mapping studies encompassed a variety of cell types from man and rat, including both tumor lines and primary cells. The scope of this survey, as well as our choices for some of the cell types tested, was motivated by our goal of developing candidate ZFPs for a variety of pro- and anti-angiogenic gene therapies. We wished to identify any constitutive accessible chromatin regions in the VEGF-A promoter, as well as those specific to medically relevant target tissues and model organisms. We observed a total of four distinct hypersensitive regions. Two of these, centered on approximately bp −550 and +1 of the VEGF-A promoter, were invariably observed in every cell type tested. Fig. 1 shows typical experimental results identifying these regions in both man (Fig. 1*A*) and rat (Fig. 1*B*). Both regions appeared as doublets when viewed at higher resolution (*e.g.* Fig. 1, *A* and *C*). The discovery of an open region centered on bp +1 was somewhat expected, as hypersensitive regions are often observed in the vicinity of sites for transcription initiation (for a review, see Ref. 43), and this region also contains conserved regulatory

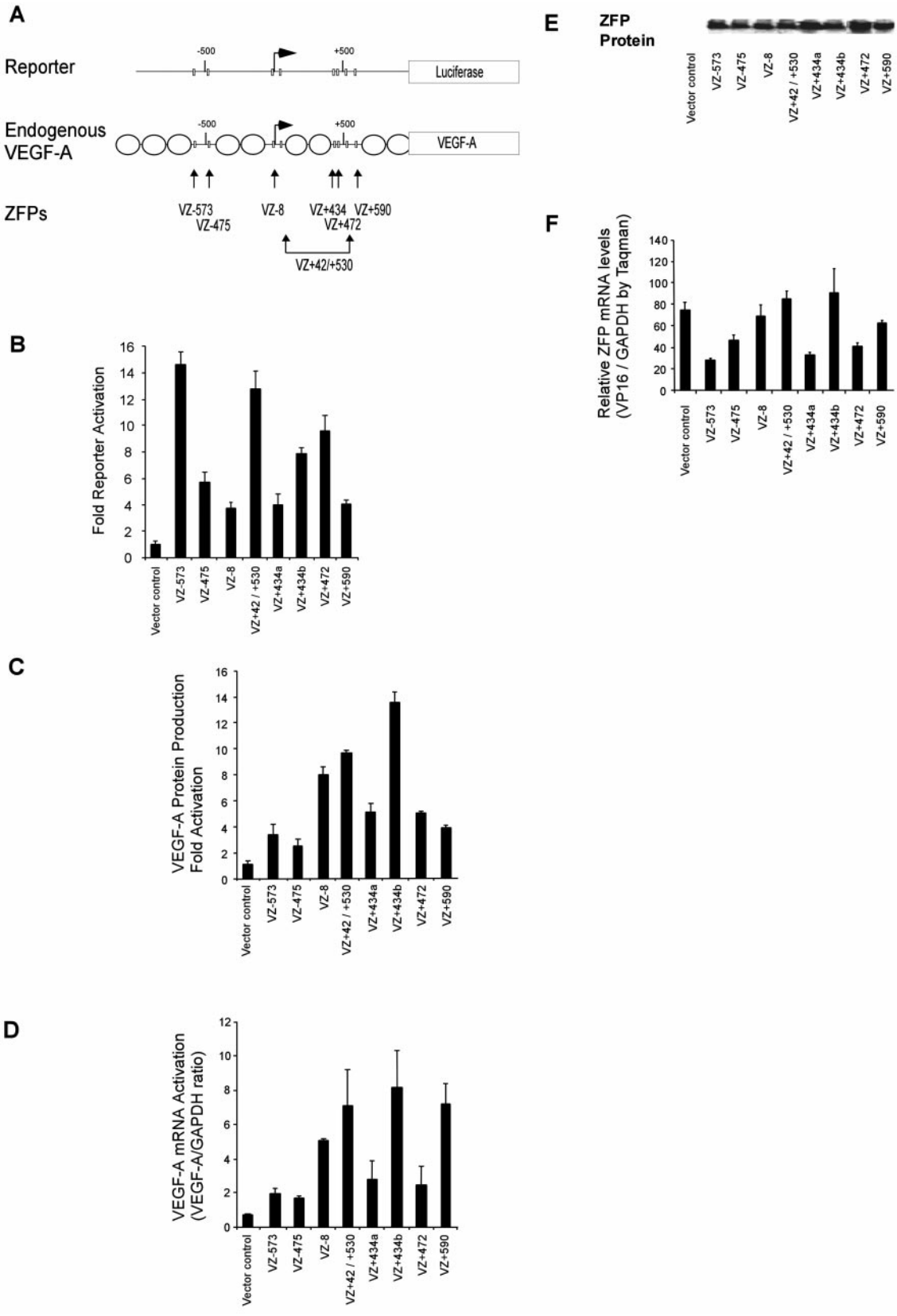

FIG. 3. **Transcriptional activation properties of ZFPs targeted to DNase I-accessible regions of VEGF-A.** *A*, schematic representation of the naked VEGF-A promoter reporter (*top*) and endogenous chromosomal (*bottom*) targets used in this experiment. Coverage of portions of the endogenous promoter with *white ovals* indicates occlusion of these regions with nucleosomes. ZFP targets are indicated by *white vertical rectangles*, and *arrows* connect each target with the name of its corresponding ZFP below. *B*, activation of the naked human VEGF-A promoter reporter by ZFP-VP16 fusions. ZFP-VP16 fusion plasmids were cotransfected with a VEGF-A reporter construct containing the luciferase gene under the control of 3.4 kilobases of the human VEGF-A promoter into HEK293 cells, and the reporter activity was assayed 40 h post-transfection as described under "Experimental Procedures." A constitutive *Renilla* luciferase construct was also cotransfected to serve as a transfection control for normalization. The fold reporter activation by the ZFPs was calculated based on the normalized luciferase reporter activity in comparison with that of a control vector encoding VP16-FLAG without ZFP. *C* and *D*, activation of the endogenous human VEGF-A gene by ZFP-VP16 fusions.

TABLE II
Zinc finger designs and apparent K_d values of the human VEGF-A-targeted ZFPs

ZFP name	Target		Finger designs (−1 to +6)	Apparent K_d
	Sequence (5′ to 3′)	Subsites (5′ to 3′)		
				nM
VZ−950	GAAGAGGACc	GACc	EKANLTR	0.18
		GAGg	RSDNLTR	
		GAAg	QRSNLVR	
VZ−573	GGGGGCGCTc	GCTc	QSSDLRR	0.63
		GGCg	QSSHLAR	
		GGGg	RSDHLSR	
VZ−475	GTGTGGGGTt	GGTt	QSSHLAR	0.35
		TGGg	RSDHLTT	
		GTGt	RSDALAR	
SP1 (−76/+527)	GGGGCGGGGg	GGGg	KTSHLRA	0.25
		GCGg	RSDELQR	
		GGGg	RSDHLSK	
VZ−8	GGGGAGGATc	GATc	TTSNLRR	2.83
		GAGg	RSSNLQR	
		GGGg	RSDHLSR	
VZ+42/+530	GCTGGGGGC t/g	GGC t/g	DRSHLTR	0.33
		GGGg	RSDHLTR	
		GCTg	QSSDLTR	
VZ+434a	GGGGGTGACc	GACc	DRSNLTR	0.14
		GGTg	TSGHLVR	
		GGGg	RSDHLSR	
VZ+434b	GGGGGTGACc	GACc	DRSNLTR	0.41
		GGTg	MSHHLSR	
		GGGg	RSDHLSR	
VZ+472	AAGGGGGAGg	GAGg	RSDNLAR	0.005
		GGGg	RSDHLSR	
		AAGg	RSDNLTQ	
VZ+590	GCAGGGGCCg	GCCg	DRSSLTR	0.23
		GGGg	RSDHLSR	
		GCAg	QSGSLTR	
VZ+892	GCTGGAGCAc	GCAc	QSGSLTR	0.24
		GGAg	QSGHLQR	
		GCTg	QSSDLTR	

elements that have been shown to be important for VEGF-A activation, including targets for SP1 and AP-2 (44). The observation in both man and rat of accessible chromatin in the −550 region was somewhat more surprising, as no regulatory elements have thus far been mapped to this area of the VEGF-A promoter. Interestingly, this region exhibits a high degree of sequence conservation across all species for which VEGF-A promoter sequence is available (man, mouse, and rat) (Fig. 1*F*, *gray trace*), which becomes more pronounced when conservation is considered in terms of regulatory element-sized sequence blocks (Fig. 1*F*, *black trace*). This suggests the possibility that as yet unidentified regulators of VEGF-A transcription may operate via binding to elements in this region. Initial studies in which a DNA fragment containing this region was fused to the promoter of a luciferase reporter indicated that this region exhibited *cis*-acting regulatory functions (data not shown). We excluded the possibility that this DNA sequence itself was a more favored substrate for DNase I digestion by performing a control mapping study using purified naked genomic DNA, which indicated no enhanced cutting of this region by DNase I (data not shown).

In addition to the constitutive hypersensitive regions found at bp −550 and +1, we identified two other stretches of accessible chromatin that were apparent in only a subset of the cells used in our studies. One of these regions encompassed ~300 bp centered on the hypoxia response element of VEGF-A and was observed in human primary skeletal muscle cells (Fig. 1*C*) and in the Hep3B cell line (data not shown). In contrast, this site was clearly not observed in HEK293 cells (Fig. 1*C*). The hypoxia response element encompasses a region of enhanced sequence conservation in the VEGF-A promoter (Fig. 1*F*) and has been shown to contain several conserved regulatory elements that are required for induction of VEGF-A by hypoxia, including a binding site for hypoxia-inducible factor 1 (38, 39, 46). A final hypersensitive region was observed ~500 bp downstream of the transcription start site in HEK293 cells (Fig. 1*D*), primary skeletal muscle cells (data not shown), and rat primary cardiac myocytes (Fig. 1*B*). Interestingly, this region contains a putative SP1-binding site and is adjacent to an alternate transcription start site (47) (Fig. 1*E*). This region also displayed the capacity to activate the expression of a reporter gene in *cis* (data not shown). In summary, these studies identified four regions of accessible chromatin within the promoter region of VEGF-A that were conserved in rat and man (Fig. 1*E*). Three of these, centered at approximately bp −550, +1, and +500 relative to the transcription start site, were found in HEK293 cells

Plasmids encoding ZFP-VP16 fusions were transfected into HEK293 cells via LipofectAMINE reagent as described under "Experimental Procedures." The control vector expressed VP16-FLAG fused with green fluorescent protein instead of ZFP. Forty hours after transfection, the culture medium and cells were harvested and assayed for endogenous VEGF-A expression. In *C*, the VEGF-A protein contents in the culture medium were measured by ELISA using a human VEGF-A ELISA kit. The VEGF-A protein production induced by the ZFPs was compared with that of the control vector. The fold activation was plotted. In *D*, the steady-state VEGF-A mRNA levels in the transfected cells was measured by quantitative RT-PCR using Taqman chemistry as described under "Experimental Procedures." The levels of VEGF-A mRNA were normalized against glyceraldehyde-3-phosphate dehydrogenase (*GAPDH*). *E*, the ZFP protein contents in the transfected cells analyzed by Western blotting using anti-FLAG antibody (Sigma), which recognizes the FLAG epitope tag of the engineered ZFPs. *F*, levels of ZFP mRNA in the transfected cells determined by Taqman and normalized against glyceraldehyde-3-phosphate dehydrogenase mRNA levels. The primers and probe were designed to recognize the sequence encoding the VP16 activation domain and FLAG tag.

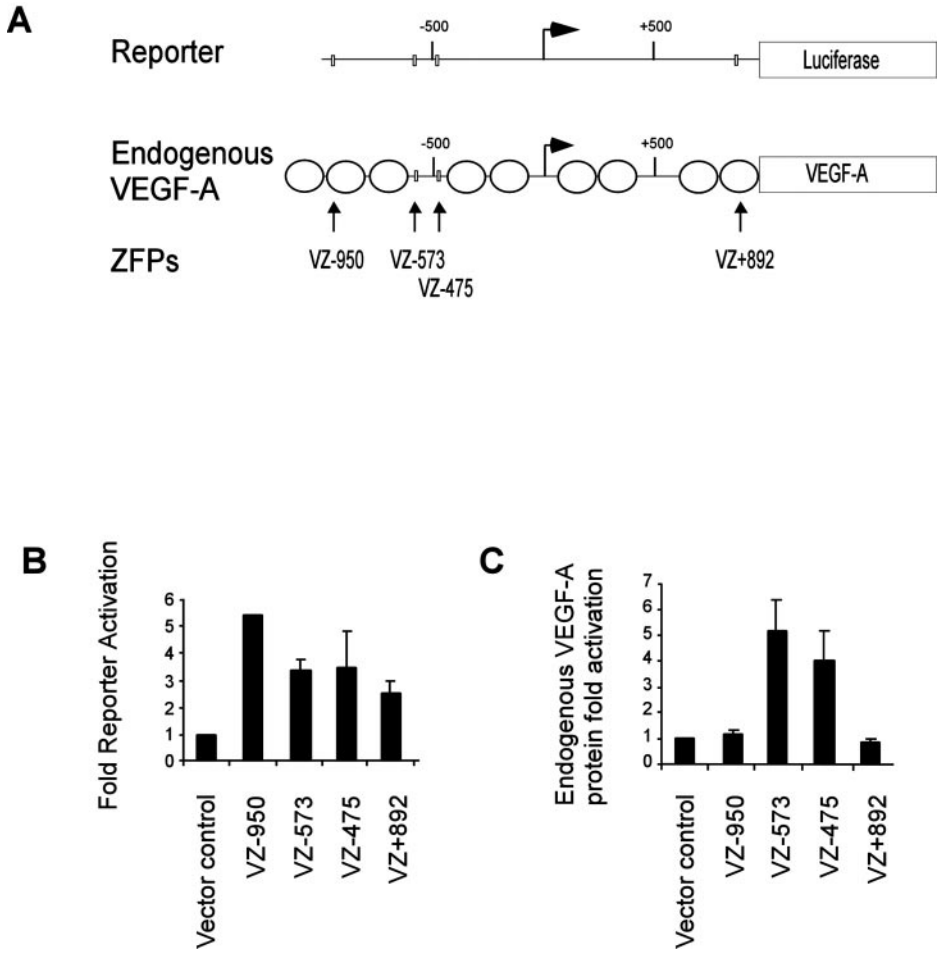

FIG. 4. **Differential behavior of ZFPs targeted to accessible and inaccessible regions of VEGF-A.** *A*, schematic representation of the naked VEGF-A promoter reporter (*top*) and endogenous chromosomal (*bottom*) targets used in this experiment. Coverage of portions of the endogenous promoter with *white ovals* indicates occlusion of these regions with nucleosomes. ZFP targets are indicated by *white vertical rectangles*, and *arrows* connect each target with the name of its corresponding ZFP below. *B*, activation of the naked human VEGF-A promoter reporter. The indicated ZFP-VP16 fusion plasmids were cotransfected with the VEGF-A-luciferase reporter construct as described under "Experimental Procedures." The fold luciferase reporter activation by the ZFPs was calculated in comparison with that of a control vector encoding VP16-FLAG without ZFP. *C*, activation of the endogenous human VEGF-A gene. Plasmids encoding the various indicated ZFP-VP16 fusions were transfected into HEK293 cells, and the VEGF-A protein contents secreted in the culture medium 40 h after transfection were measured by ELISA as described for Fig. 3*C*. The VEGF-A protein production induced by the ZFPs was compared with that of the control vector, and the -fold activation was plotted.

and were targeted for further studies with designed ZFPs.

Design and Biochemical Characterization of ZFPs Targeted to Open Chromatin Regions of VEGF-A—Design and selection studies of zinc finger-DNA recognition have yielded a diverse collection of fingers with characterized triplet specificities (4–14, 16, 48, 49). Collectively, these fingers provide a "directory" of triplet-binding modules that may be mixed and matched to obtain multifinger proteins with the desired binding properties. In particular, we have found that when care is taken to preserve finger context, the preferred targets of the resultant ZFPs are typically a composite of the component finger triplet specificities. Using this approach, we have designed ZFPs that recognize targets within the −550, +1, and +500 open chromatin regions observed in HEK293 cells (Fig. 2*D*) and assembled genes for these ZFPs. We also included two control ZFPs targeted to sites outside of the hypersensitive regions. The designs for our ZFPs are shown in Table II with each finger design indicated by the amino acid sequence of positions "−1" through "+6" of its α-helix. We have named the ZFPs according to their target location relative to the transcription start site of VEGF-A. Thus, the first bases in the target sequences of VZ−475 and VZ+590 lie 475 base pairs upstream and 590 nucleotides downstream, respectively, of the principal site of transcription initiation. One of our designs has two target sites in this region and so has been given a complex name to reflect this fact (VZ+42/+530). Where there are multiple ZFPs targeted to a given sequence, this is indicated by the use of a lowercase letter suffix at the end of each name to distinguish between alternate ZFP designs.

Genes for our ZFPs were assembled using previously described methods (17), and each protein was expressed in recombinant form (Fig. 2, *A-C*). We then characterized the DNA-binding affinity of each ZFP using a gel shift assay. Procedures for these studies were similar to those described previously (17) (for details, see "Experimental Procedures"). We found that our designed ZFPs exhibited a range of apparent K_d values for their intended DNA targets from 0.005 to 3 nM (Fig. 2*E*). For comparison, under these conditions, SP1, the parent ZFP for our designs, exhibited an apparent K_d of 0.25 nM for its DNA target (Fig. 2*E*). These studies demonstrated that each designed ZFP recognizes its target site with high affinity.

Activation of the Human VEGF-A Gene Promoter by ZFPs—We chose to use HEK293 cells for our initial studies of VEGF-A activation with our designed ZFPs since these cells offered an especially favorable combination of high transfectability (typically >70%) and low background expression levels of VEGF-A. We first tested for the ability of the designed ZFPs to activate the VEGF-A promoter reporter. The ZFPs were fused to the minimal activation domain of the herpes simplex virus transcription factor VP16 with a C-terminal FLAG epitope tag and tested for their activity in cells. To test for human VEGF-A gene promoter activity, a reporter plasmid was constructed to contain firefly luciferase gene under the control of the human VEGF-A promoter. When cotransfected transiently with the reporter plasmid, all of the designed ZFP-VP16 fusions were able to activate the reporter (Fig. 3*B*). The level of activation ranged between 3- and 15-fold. The activation was ZFP-dependent; a fusion of green fluorescent protein (50) with VP16 was unable to activate the reporter. This result showed that all of the designed ZFPs were active on a naked DNA template. There also appeared to be no strong correlation between the binding affinity of each ZFP and its capacity to transiently activate the VEGF-A promoter reporter from distant sites in the locus.

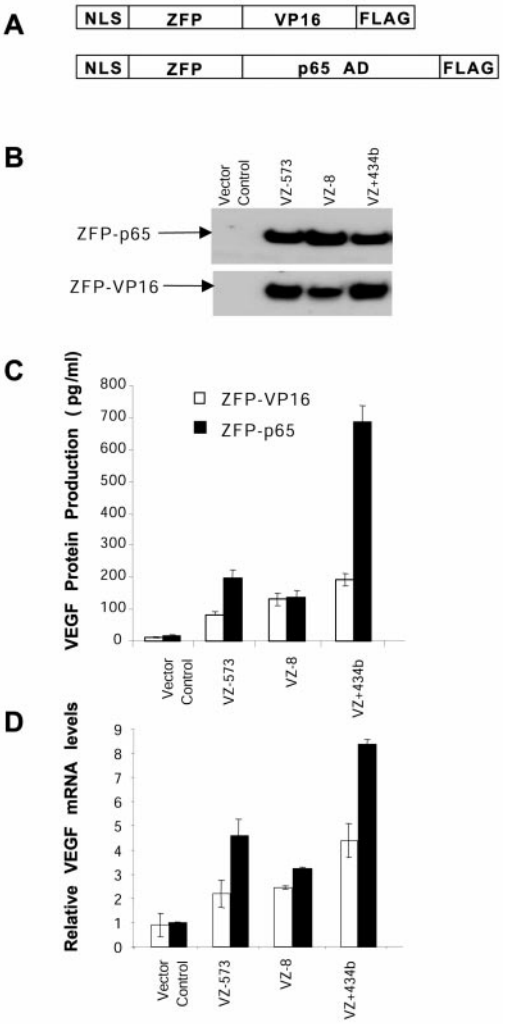

FIG. 5. **Activation of the endogenous human VEGF-A gene by ZFP with different activation domains.** Various ZFPs were fused with VP16 (□) or the activation domain (*AD*) from NF-κB (p65) (■), both with a C-terminal FLAG tag. Their activities were tested as described in the legend to Fig. 3 and compared. *A*, shown is a scheme of the VEGF-A-targeted VP16 and p65 activation domain-linked ZFP fusions. *B*, the ZFP protein contents in the transfected cells were analyzed by Western blotting using anti-FLAG antibody. *C*, the VEGF-A protein contents in the culture medium were measured by ELISA. *D*, the steady-state VEGF-A mRNA levels in the transfected cells were measured by Taqman. *NLS*, nuclear localization signal.

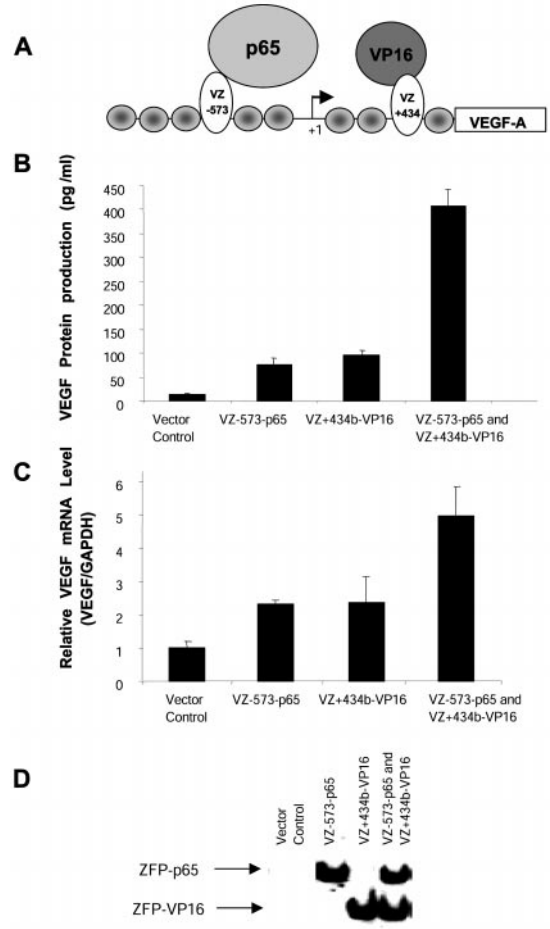

FIG. 6. **Cooperativity between ZFPs with different activation domains in VEGF-A gene activation.** Plasmids containing different ZFP-activation domain fusions were cotransfected at a 1:1 ratio into HEK293 cells. Endogenous VEGF-A activation was measured 40 h after transfection. *A*, shown is a scheme of the experiment. *B*, the VEGF-A protein contents in the culture medium were assayed by ELISA. *C*, the VEGF-A mRNA levels in the transfected cells were measured by Taqman. *D*, the ZFP protein contents in the transfected cells were analyzed by Western blotting using anti-FLAG antibody. *GAPDH*, glyceraldehyde-3-phosphate dehydrogenase.

Transcriptional Activation of the Endogenous Human VEGF-A Gene Using ZFPs—To test whether these ZFP-VP16 fusions were also active in regulating VEGF-A gene transcription from the endogenous chromosomal locus, the designed ZFP-VP16 fusions were transiently transfected into HEK293 cells, and their effect on endogenous VEGF-A gene expression was analyzed. HEK293 cells produce relatively low levels of VEGF-A in the absence of any ZFP constructs. As shown in Fig. 3*C*, expression of the ZFP-VP16 fusions targeted to the open chromatin regions resulted in the secretion of elevated levels of VEGF-A into the medium as determined by ELISA. The range of activation varied between 2- and 15-fold, with ZFP VZ+434b being the most active. The increased VEGF-A protein production induced by ZFP was correlated with a 2–10-fold increase in the level of VEGF-A mRNA as determined by quantitative PCR (Fig. 3*D*). In contrast to their variable activities, the ZFPs were found to be expressed to similar levels as determined by Western blotting (Fig. 3*E*) and by Taqman for mRNA expression (Fig. 3*F*). Therefore, the differential activity of the ZFP-VP16 fusions most likely is not related to differential ZFP expression.

We also compared the behavior of ZFPs targeted to the accessible regions of VEGF-A with two ZFPs targeted to inaccessible regions. Data for these studies are shown in Fig. 4. Whereas all four ZFPs activated the naked reporter construct to approximately equal levels, a clear discrepancy was seen regarding activity against the endogenous VEGF-A gene. The accessible region-targeted ZFPs activated VEGF-A by factors of 4–5, whereas the ZFPs targeted to sites outside of the accessible regions showed no appreciable increase in VEGF-A expression levels.

Activation of the Human VEGF-A Gene by ZFPs Fused with Different Activation Domains—To achieve a higher level of VEGF-A activation by ZFPs in human cells, we tested the performance of other activation domains against that achieved by VP16 (data not shown). We found that the activation domain from the p65 subunit of NF-κB offered higher levels of activation when tested using several of our ZFPs (Fig. 5). In this experiment, some ZFP-p65 fusions, *e.g.* ZFP VZ+434b, induced a VEGF-A protein accumulation that was 3–4-fold higher than that induced by ZFP-VP16 fusions (Fig. 5*C*), although the ZFP-p65 fusion proteins were expressed and accumulated in cells to similar levels as the ZFP-VP16 fusions (Fig. 5*B*). The higher level of ZFP-p65 fusion-induced VEGF-A protein production

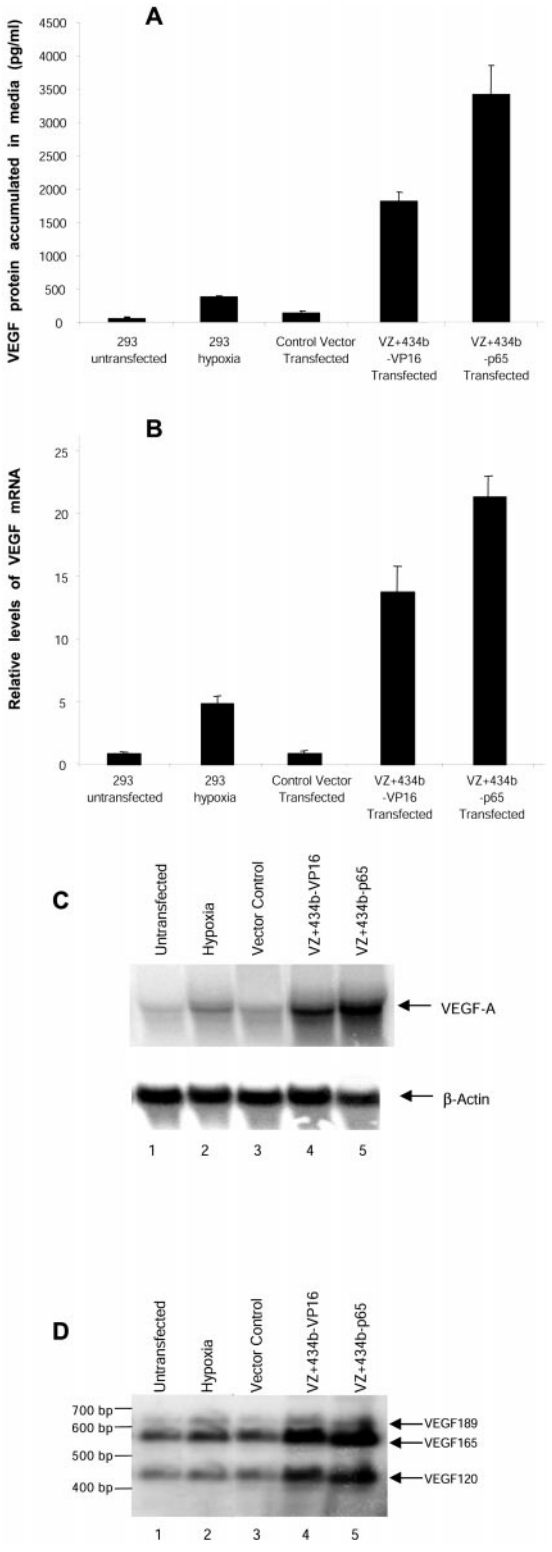

FIG. 7. **Activation of the endogenous human VEGF-A gene by ZFP VZ+434b and by hypoxia.** HEK293 cells grown in 150-mm dishes either were transfected with plasmids encoding ZFP VZ+434b fused with VP16 or p65 or with a control vector expressing no ZFP or were grown under hypoxic conditions (0.5% oxygen) for 24 h. Endogenous VEGF-A gene activation was measured as described in the legend to Fig. 3 and compared. *A*, the VEGF-A protein contents in the culture medium were measured by ELISA. *B*, the steady-state VEGF-A mRNA levels in the cells were measured by Taqman and normalized against 18 S RNA. *C*, the VEGF-A mRNA levels were detected by Northern hybridization using a ^{32}P-labeled VEGF-A-165 cDNA probe. *D*, the splice variants for VEGF-A were analyzed by RT-PCR and detected by Southern hybridization using a ^{32}P-labeled VEGF-A-165 cDNA probe as described under "Experimental Procedures."

was consistent with a higher level of VEGF-A mRNA transcription as determined by Taqman analysis (Fig. 5*D*). Interestingly, for some ZFPs such as VZ−8, the p65 and VP16 fusions displayed similar activities, suggesting that VP16 and p65 may have distinct target location-dependent activation mechanisms.

Cooperation between ZFPs for Activation of the Human VEGF-A Gene—The availability of a set of activating ZFPs targeted to diverse regions of the VEGF-A gene promoter and fused to different activation domains provided an opportunity to investigate whether combinations of ZFPs with different activation domains could achieve an enhanced activation of VEGF-A gene expression. To test this possibility, various ZFP-VP16 and ZFP-p65 fusions were cotransfected into HEK293 cells and tested for VEGF-A activation by ELISA and Taqman. As shown in Fig. 6, ZFPs VZ+434b-VP16 and VZ−573a-p65 individually activated VEGF-A protein production in HEK293 cells by 8- and 6-fold, respectively. However, when they were cotransfected at a 1:1 ratio into the cells, the level of VEGF-A gene activation was enhanced (30-fold by ELISA) compared with the levels induced by each individual ZFP. A similar cooperation between ZFPs VZ+434b-p65 and VZ−573a-VP16 was also observed (data not shown).

Comparison with Levels of VEGF-A Produced by Hypoxia—To assess how our ZFP-activated levels of VEGF-A expression compared with the levels produced by physiologically relevant processes, we compared VEGF-A production induced by ZFPs with that induced by hypoxia. For many ZFPs tested, *e.g.* ZFP VZ+434b, we found that the ZFPs were capable of activating VEGF-A expression to a level higher than that induced by hypoxia. As shown in Fig. 7, HEK293 cells growing under hypoxic conditions had a 5-fold higher steady-state VEGF-A mRNA level than under normoxic conditions (Fig. 7*B*) and accumulated VEGF-A protein to nearly 400 pg/ml in medium (a 10-fold increase) (Fig. 7*A*). ZFP VZ+434b with a p65 activation domain was able to activate the VEGF-A gene 5–10 times further than that induced by hypoxia with an accumulation of VEGF-A protein in the culture medium to nearly 4000 pg/ml (Fig. 7*A*) and a 20-fold increase in the VEGF-A mRNA level (Fig. 7*B*). This observation was also confirmed by Northern blot analysis (Fig. 7*C*).

Activation of Multiple Splice Variants Using a Single ZFP—Several splice variants of human VEGF-A have been discovered, each one comprising a specific exon addition (24). The major forms produce polypeptides with 121, 165, 189, and 206 amino acids, although VEGF-A-206 is rarely expressed and has been detected only in fetal liver. Because our ZFPs activated gene transcription from the natural promoter on the chromosome, we predicted that they would activate all of the different VEGF-A transcripts equally, preserving their relative proportions. To test this notion, we analyzed the ability of ZFP VZ+434b to activate multiple transcripts from the same promoter. To distinguish the various splice variants, RT-PCR was performed using primers flanking the splice regions and producing distinct PCR products for each splice variant. The PCR products were then analyzed by Southern hybridization using a VEGF-A-165 probe. Three splice variants, VEGF-A-189, VEGF-A-165, and VEGF-A-121, were detected in HEK293 cells, with VEGF-A-165 being the predominant form. As demonstrated in Fig. 7*D*, the introduction of a single ZFP, VZ+434b as either a VP16 or p65 fusion, resulted a proportional increase in all of the splice variants.

DISCUSSION

In this study, we have successfully designed a panel of ZFPs that bind with high affinity to diverse DNA sequences present within the VEGF-A locus (Fig. 2) and that are capable of

activating expression of the endogenous human chromosomal VEGF-A gene (Figs. 3–7). Our experimental approach incorporated information regarding the chromatin structure of the VEGF-A locus such that proteins were designed to sequences present within the DNase I-hypersensitive regions (Fig. 1), and this contributed to the large number of locations that we have identified from which designed transcription factors may activate VEGF-A (Figs. 3 and 4) relative to single targets described in previous studies (16–18). We propose that ZFP targeting strategies that incorporate information regarding chromatin structure will provide a more efficient means for identifying artificial transcription factors capable of specifically regulating endogenous genes compared with strategies based on ZFP design principles alone. We found that several of these designed ZFPs are quite potent, yielding VEGF-A levels that exceed those induced by hypoxia (Fig. 7). We speculate that the regulation of multiple VEGF-A splice variants will be of utility in somatic gene therapy approaches to cardiovascular disease (51–56).

Our panel of artificial transcription factors targeted to diverse sites in VEGF-A provides a unique tool for assessing the structural determinants of transcriptional activation at an endogenous locus, and several of our results may bear the signature of the transcriptional effects of chromatin structure. We found, for example, that our panel of ZFPs exhibits quite different patterns of activation when tested using the endogenous VEGF-A locus *versus* a naked promoter reporter construct (Fig. 3, compare *B* and *C*). They also differ depending on whether the site is within a DNase I-accessible region or not (Fig. 4). Furthermore, we observed that the ability of the p65 activation domain to outperform VP16 also varies in a target site-dependent manner, with relative activation levels varying over a factor of 3 depending on the location of the ZFP target within the VEGF-A locus (Fig. 5). These effects highlight the role of structural context that is imposed by chromatin and the binding of other regulatory proteins on the capacity of transcription factors to activate an endogenous locus and also reemphasize the distinct regulatory and steric requirements of different activation domains to achieve optimal performance.

The capacity to generate a panel of designed transcription factors targeted to diverse sites in an endogenous locus also provides practical advantages in a variety of applications. In studying the effects of up- or down-regulation of a target locus, for example, conclusions regarding gene function will be strongest if a given effect is observed repeatedly using multiple different regulators. In addition, for potential medical uses, the availability of multiple ZFP candidates provides a greater likelihood of finding one that yields optimal benefits with minimal side effects. Perhaps the most exciting possibilities for use of these proteins, however, lie in the study of transcriptional regulation. For example, the ability to target multiple activation domains to arbitrary sites in the same locus may have applications in the study of synergy. In this study, we have taken the first steps to examine this issue and have demonstrated enhanced effects on transcriptional activation mediated by cotransfected VP16 and p65 activation domain-bearing ZFPs. It seems reasonable to speculate that, by using larger combinations of appropriately targeted functional domains, our ZFPs may offer the prospect for total reconstitution of activation processes using completely defined components.

An additional observation of these studies is that ZFPs fused with the 268-amino acid activation domain of p65 (42) activate the endogenous VEGF-A gene as well as or better than the 78-amino acid activation domain of the herpes simplex virus VP16 (41). Although both VP16 and NF-κB p65 are strong acidic activation domains and share certain functional features (for example, recruitment of the ARC/DRIP complex and facilitated assembly of a preinitiation complex on promoter DNA (57, 58)), differences in their transactivation mechanism have been reported. For example, the histone acetyltransferase activity of p300 has been demonstrated to be necessary for activation by NF-κB, but less essential for activation by VP16 (59, 60). It is possible that the local availability of p300 or other coactivators in the endogenous VEGF-A locus may account for the differences we observed.

Finally, we have observed that our designed ZFPs up-regulate each major splice variant of VEGF-A proportionally. This is important because recent studies suggest that proper isoform balance is crucial for VEGF-A function (27, 28). In particular, the 165, 189, and 206 splice variants have increasingly stronger heparin-binding domains, which help them bind to the extracellular matrix and are involved in presentation to VEGF-A receptors. The heparin-binding ability is a critical determinant of VEGF-A potency, resulting in different biological activities for different splice variants. Currently, most VEGF-A gene therapy trials involve the application of just a single VEGF-A splice variant protein or cDNA (51–55), and it has been suggested that an ideal gene therapy agent should be able to recapitulate natural ratios of various different VEGF-A isoforms. Activation of VEGF-A using our designed ZFPs may therefore offer advantages in this regard, and VEGF-A-specific ZFPs could provide key components of the next generation of pro-angiogenic gene therapy agents.

Acknowledgments—We thank Reed Hickey and Frank Giordano for providing key protocols and advice for the rat neonatal cardiac myocyte preparations; Brian Johnstone, Priya Sreenivasan, and Yolanda Santiago for helpful discussions and assistance with the mapping of DNase I-accessible regions; Michelle Ha for expert technical support in early cell culture studies; and Monica Miller, Katherine Pasquetti, Anna Vincent, Damon Toroian, and Brad Campos for assembly and initial testing of ZFP constructs. We are also grateful to Edward Lanphier, Peter Bluford, and Carl Pabo for encouragement and support.

REFERENCES

1. Kim, J. S., Kim, J., Cepek, K. L., Sharp, P. A., and Pabo, C. O. (1997) *Proc. Natl. Acad. Sci. U. S. A.* **94,** 3616–3620
2. Chatterjee, S., and Struhl, K. (1995) *Nature* **374,** 820–822
3. Klages, N., and Strubin, M. (1995) *Nature* **374,** 822–823
4. Jamieson, A. C., Kim, S. H., and Wells, J. A. (1994) *Biochemistry* **33,** 5689–5695
5. Jamieson, A. C., Wang, H., and Kim, S. H. (1996) *Proc. Natl. Acad. Sci. U. S. A.* **93,** 12834–12839
6. Rebar, E. J., and Pabo, C. O. (1994) *Science* **263,** 671–673
7. Rebar, E. J., Greisman, H. A., and Pabo, C. O. (1996) *Methods Enzymol.* **267,** 129–149
8. Desjarlais, J. R., and Berg, J. M. (1992) *Proteins Struct. Funct. Genet.* **13,** 272
9. Desjarlais, J. R., and Berg, J. M. (1992) *Proteins Struct. Funct. Genet.* **12,** 101–104
10. Desjarlais, J. R., and Berg, J. M. (1993) *Proc. Natl. Acad. Sci. U. S. A.* **90,** 2256–2260
11. Greisman, H. A., and Pabo, C. O. (1997) *Science* **275,** 657–661
12. Choo, Y., and Klug, A. (1994) *Proc. Natl. Acad. Sci. U. S. A.* **91,** 11168–11172
13. Choo, Y., and Klug, A. (1994) *Proc. Natl. Acad. Sci. U. S. A.* **91,** 11163–11167
14. Segal, D. J., Dreier, B., Beerli, R. R., and Barbas, C. F., III (1999) *Proc. Natl. Acad. Sci. U. S. A.* **96,** 2758–2763
15. Liu, Q., Segal, D. J., Ghiara, J. B., and Barbas, C. F., III (1997) *Proc. Natl. Acad. Sci. U. S. A.* **94,** 5525–5530
16. Bartsevich, V. V., and Juliano, R. L. (2000) *Mol. Pharmacol.* **58,** 1–10
17. Zhang, L., Spratt, S. K., Liu, Q., Johnstone, B., Qi, H., Raschke, E. E., Jamieson, A. C., Rebar, E. J., Wolffe, A. P., and Case, C. C. (2000) *J. Biol. Chem.* **275,** 33850–33860
18. Beerli, R. R., Dreier, B., and Barbas, C. F., III (2000) *Proc. Natl. Acad. Sci. U. S. A.* **97,** 1495–1500
19. Archer, T. K., Lefebvre, P., Wolford, R. G., and Hager, G. L. (1992) *Science* **255,** 1573–1576
20. Tse, C., Sera, T., Wolffe, A. P., and Hansen, J. C. (1998) *Mol. Cell. Biol.* **18,** 4629–4638
21. Wolffe, A. P., and Hayes, J. J. (1999) *Nucleic Acids Res.* **27,** 711–720
22. Yancopoulos, G. D., Davis, S., Gale, N. W., Rudge, J. S., Wiegand, S. J., and Holash, J. (2000) *Nature* **407,** 242–248
23. Flamme, I., Frohlich, T., von Reutern, M., Kappel, A., Damert, A., and Risau, W. (1997) *Mech. Dev.* **63,** 51–60
24. Ferrara, N. (1999) *J. Mol. Med.* **77,** 527–543
25. Ferrara, N., Carver-Moore, K., Chen, H., Dowd, M., Lu, L., O'Shea, K. S., Powell-Braxton, L., Hillan, K. J., and Moore, M. W. (1996) *Nature* **380,** 439–442

26. Carmeliet, P., Ferreira, V., Breier, G., Pollefeyt, S., Kieckens, L., Gertsenstein, M., Fahrig, M., Vandenhoeck, A., Harpal, K., Eberhardt, C., Declercq, C., Pawling, J., Moons, L., Collen, D., Risau, W., and Nagy, A. (1996) *Nature* **380,** 435–439
27. Carmeliet, P., Ng, Y. S., Nuyens, D., Theilmeier, G., Brusselmans, K., Cornelissen, I., Ehler, E., Kakkar, V. V., Stalmans, I., Mattot, V., Perriard, J. C., Dewerchin, M., Flameng, W., Nagy, A., Lupu, F., Moons, L., Collen, D., D'Amore, P. A., and Shima, D. T. (1999) *Nat. Med.* **5,** 495–502
28. Grunstein, J., Masbad, J. J., Hickey, R., Giordano, F., and Johnson, R. S. (2000) *Mol. Cell. Biol.* **20,** 7282–7291
29. Damert, A., Ikeda, E., and Risau, W. (1997) *Biochem. J.* **327,** 419–423
30. Diaz, B. V., Lenoir, M. C., Ladoux, A., Frelin, C., Demarchez, M., and Michel, S. (2000) *J. Biol. Chem.* **275,** 642–650
31. Cohen, T., Nahari, D., Cerem, L. W., Neufeld, G., and Levi, B. Z. (1996) *J. Biol. Chem.* **271,** 736–741
32. Chua, C. C., Hamdy, R. C., and Chua, B. H. (1998) *Free Radic. Biol. Med.* **25,** 891–897
33. Salimath, B., Marme, D., and Finkenzeller, G. (2000) *Oncogene* **19,** 3470–3476
34. Ladoux, A., and Frelin, C. (1994) *Biochem. Biophys. Res. Commun.* **204,** 794–798
35. Ryuto, M., Ono, M., Izumi, H., Yoshida, S., Weich, H. A., Kohno, K., and Kuwano, M. (1996) *J. Biol. Chem.* **271,** 28220–28228
36. Kimura, H., Weisz, A., Ogura, T., Hitomi, Y., Kurashima, Y., Hashimoto, K., D'Acquisto, F., Makuuchi, M., and Esumi, H. (2001) *J. Biol. Chem.* **276,** 2292–2298
37. Kimura, H., Weisz, A., Kurashima, Y., Hashimoto, K., Ogura, T., D'Acquisto, F., Addeo, R., Makuuchi, M., and Esumi, H. (2000) *Blood* **95,** 189–197
38. Levy, A. P., Levy, N. S., Wegner, S., and Goldberg, M. A. (1995) *J. Biol. Chem.* **270,** 13333–13340
39. Liu, Y., Cox, S. R., Morita, T., and Kourembanas, S. (1995) *Circ. Res.* **77,** 638–643
40. Forsythe, J. A., Jiang, B. H., Iyer, N. V., Agani, F., Leung, S. W., Koos, R. D., and Semenza, G. L. (1996) *Mol. Cell. Biol.* **16,** 4604–4613
41. Sadowski, I., Ma, J., Triezenberg, S., and Ptashne, M. (1988) *Nature* **335,** 563–564
42. Ruben, S. M., Dillon, P. J., Schreck, R., Henkel, T., Chen, C. H., Maher, M., Baeuerle, P. A., and Rosen, C. A. (1991) *Science* **251,** 1490–1493
43. Gross, D. S., and Garrard, W. T. (1988) *Annu. Rev. Biochem.* **57,** 159–197
44. Milanini, J., Vinals, F., Pouyssegur, J., and Pages, G. (1998) *J. Biol. Chem.* **273,** 18165–18172
45. Grant, R. A., Rould, M. A., Klemm, J. D., and Pabo, C. O. (2000) *Biochemistry* **39,** 8187–8192
46. Ikeda, E., Achen, M. G., Breier, G., and Risau, W. (1995) *J. Biol. Chem.* **270,** 19761–19766
47. Akiri, G., Nahari, D., Finkelstein, Y., Le, S. Y., Elroy-Stein, O., and Levi, B. Z. (1998) *Oncogene* **17,** 227–236
48. Desjarlais, J. R., and Berg, J. M. (1992) *Proc. Natl. Acad. Sci. U. S. A.* **89,** 7345–7349
49. Elrod-Erickson, M., Benson, T. E., and Pabo, C. O. (1998) *Structure* **6,** 451–464
50. Chalfie, M., Tu, Y., Euskirchen, G., Ward, W. W., and Prasher, D. C. (1994) *Science* **263,** 802–805
51. Rosengart, T. K., Lee, L. Y., Patel, S. R., Kligfield, P. D., Okin, P. M., Hackett, N. R., Isom, O. W., and Crystal, R. G. (1999) *Ann. Surg.* **230,** 466–470
52. Rosengart, T. K., Lee, L. Y., Patel, S. R., Sanborn, T. A., Parikh, M., Bergman, G. W., Hachamovitch, R., Szulc, M., Kligfield, P. D., Okin, P. M., Hahn, R. T., Devereux, R. B., Post, M. R., Hackett, N. R., Foster, T., Grasso, T. M., Lesser, M. L., Isom, O. W., and Crystal, R. G. (1999) *Circulation* **100,** 468–474
53. Hendel, R. C., Henry, T. D., Rocha-Singh, K., Isner, J. M., Kereiakes, D. J., Giordano, F. J., Simons, M., and Bonow, R. O. (2000) *Circulation* **101,** 118–121
54. Esakof, D. D., Maysky, M., Losordo, D. W., Vale, P. R., Lathi, K., Pastore, J. O., Symes, J. F., and Isner, J. M. (1999) *Hum. Gene Ther.* **10,** 2307–2314
55. Isner, J. M., Pieczek, A., Schainfeld, R., Blair, R., Haley, L., Asahara, T., Rosenfield, K., Razvi, S., Walsh, K., and Symes, J. F. (1996) *Lancet* **348,** 370–374
56. Isner, J. M., Baumgartner, I., Rauh, G., Schainfeld, R., Blair, R., Manor, O., Razvi, S., and Symes, J. F. (1998) *J. Vasc. Surg.* **28,** 964–973
57. Naar, A. M., Beaurang, P. A., Zhou, S., Abraham, S., Solomon, W., and Tjian, R. (1999) *Nature* **398,** 828–832
58. Rachez, C., Lemon, B. D., Suldan, Z., Bromleigh, V., Gamble, M., Naar, A. M., Erdjument-Bromage, H., Tempst, P., and Freedman, L. P. (1999) *Nature* **398,** 824–828
59. Kraus, W. L., Manning, E. T., and Kadonaga, J. T. (1999) *Mol. Cell. Biol.* **19,** 8123–8135
60. Li, J., O'Malley, B. W., and Wong, J. (2000) *Mol. Cell. Biol.* **20,** 2031–2042
61. Pavletich, N. P., and Pabo, C. O. (1991) *Science* **252,** 809–817